12-15-2016

An RB-EZH2 Complex Mediates Silencing of Repetitive DNA Sequences

Charles A. Ishak
London Regional Cancer Program

Aren E. Marshall
London Regional Cancer Program

Daniel T. Passos
London Regional Cancer Program

Carlee R. White
Children's Health Research Institute, London, ON

Seung J. Kim
London Regional Cancer Program

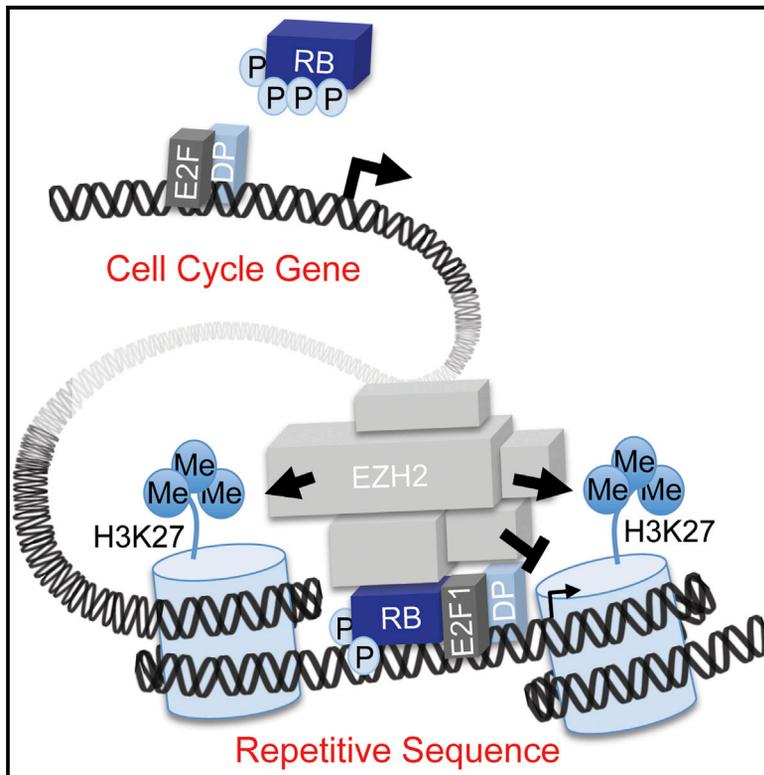*See next page for additional authors*

Authors

Charles A. Ishak, Aren E. Marshall, Daniel T. Passos, Carlee R. White, Seung J. Kim, Matthew J. Cecchini, Sara Ferwati, William A. MacDonald, Christopher J. Howlett, Ian D. Welch, Seth M. Rubin, Mellissa R.W. Mann, and Frederick A. Dick

An RB-EZH2 Complex Mediates Silencing of Repetitive DNA Sequences

Graphical Abstract

Authors

Charles A. Ishak, Aren E. Marshall,
Daniel T. Passos, ..., Seth M. Rubin,
Mellissa R.W. Mann, Frederick A. Dick

Correspondence

fdick@uwo.ca

In Brief

Ishak et al. discover that the retinoblastoma protein extensively occupies and represses expression of tandem and interspersed genomic repeats in somatic cells. RB-EZH2 recruitment to repeats establishes H3K27me3-dependent repression, and its loss permits lymphomagenesis in gene-targeted mice.

Highlights

- The retinoblastoma protein occupies repetitive sequences in somatic cells

- RB-EZH2 is required for H3K27me3 deposition at repeats and repression

- Loss of repeat repression by RB is associated with cancer susceptibility

Accession Numbers

GSE85640

CrossMark

CellPress

An RB-EZH2 Complex Mediates Silencing of Repetitive DNA Sequences

Charles A. Ishak,[1,3] Aren E. Marshall,[1,3] Daniel T. Passos,[1,3] Carlee R. White,[2,3] Seung J. Kim,[1,3] Matthew J. Cecchini,[1,4] Sara Ferwati,[1,3] William A. MacDonald,[5,6] Christopher J. Howlett,[4] Ian D. Welch,[7] Seth M. Rubin,[8] Mellissa R.W. Mann,[5,6] and Frederick A. Dick[1,2,3,9,*]

[1]London Regional Cancer Program, London, ON N6A 4L6, Canada
[2]Children's Health Research Institute, London, ON N6A 4L6, Canada
[3]Department of Biochemistry
[4]Department of Pathology and Laboratory Medicine
Western University, London, ON N6A 3K7, Canada
[5]Magee-Womens Research Institute, Pittsburgh, PA 15213, USA
[6]Department of Obstetrics, Gynecology, and Reproductive Sciences, University of Pittsburgh, Pittsburgh, PA 15260, USA
[7]Animal Care Services, University of British Columbia, Vancouver, BC V6T1Z4, Canada
[8]Department of Chemistry and Biochemistry, University of California, Santa Cruz, Santa Cruz, CA 95064, USA
[9]Lead Contact
*Correspondence: fdick@uwo.ca
http://dx.doi.org/10.1016/j.molcel.2016.10.021

SUMMARY

Repetitive genomic regions include tandem sequence repeats and interspersed repeats, such as endogenous retroviruses and LINE-1 elements. Repressive heterochromatin domains silence expression of these sequences through mechanisms that remain poorly understood. Here, we present evidence that the retinoblastoma protein (pRB) utilizes a cell-cycle-independent interaction with E2F1 to recruit enhancer of zeste homolog 2 (EZH2) to diverse repeat sequences. These include simple repeats, satellites, LINEs, and endogenous retroviruses as well as transposon fragments. We generated a mutant mouse strain carrying an F832A mutation in *Rb1* that is defective for recruitment to repetitive sequences. Loss of pRB-EZH2 complexes from repeats disperses H3K27me3 from these genomic locations and permits repeat expression. Consistent with maintenance of H3K27me3 at the *Hox* clusters, these mice are developmentally normal. However, susceptibility to lymphoma suggests that pRB-EZH2 recruitment to repetitive elements may be cancer relevant.

INTRODUCTION

Repetitive genomic regions comprise approximately 50% of the human genome (Lander et al., 2001). These repetitive elements include tandem repeats, such as satellite sequences that underpin the heterochromatin at centromeres, in addition to interspersed repeats that are capable of transposition (Slotkin and Martienssen, 2007). Expression of repetitive elements poses a mutagenic threat to the host through multiple possible aberrations (Mager and Stoye, 2015). For example, de-repres-

sion of satellite repeats disrupts organization of centromeric heterochromatin and coincides with defects in chromosome segregation and meiosis (Slotkin and Martienssen, 2007). At the transcriptional level, de-repressed repeat sequences can serve as alternate enhancers or promoters that permit "read-through" transcription and *cis*-activation of proximal genes, including proto-oncogenes that have been established as initiating events in human lymphomas (Lamprecht et al., 2010). More recently, sequencing-based studies demonstrate that re-integration of activated mobile repetitive elements can generate cancer-relevant mutations in pre-malignant lesions that precede various human cancers (Helman et al., 2014; Iskow et al., 2010; Lamprecht et al., 2010; Lee et al., 2012; Lock et al., 2014). Likewise, re-integration of activated satellites expands centromere repeats and can fuel cancer cell growth (Bersani et al., 2015). The frequent co-occurrence of repetitive element reactivation with genome instability suggests that the antagonism of repeat silencing may be achieved through mechanisms commonly employed to initiate tumorigenesis. Recent evidence of p53-mediated transposon repression indicates that this may indeed be the case (Leonova et al., 2013; Wylie et al., 2016). Thus, any potential contribution of repetitive sequences to cancer initiation must ultimately be mitigated through transcriptional silencing. Understanding how silencing is achieved is fundamental to understanding how cancer-initiating mechanisms may circumvent this facet of genome regulation.

Repetitive elements are transcriptionally repressed by DNA methylation and histone tail modifications (Schlesinger and Goff, 2015). Sustained repression of repetitive elements during periods of genome-wide DNA hypomethylation in early embryogenesis has stimulated investigation of histone-dependent repression mechanisms in embryonic stem cells (ESCs) (Leung and Lorincz, 2012; Levin and Moran, 2011). Repetitive sequences in ESCs are enriched for H3K9me2/3, H4K20me3, and H3K27me3 (Day et al., 2010). Upon loss of DNA methylation, H3K27me3 expands to maintain silencing of

interspersed and tandem repeat sequences (Walter et al., 2016). Following genetic ablation of H3K9 histone methyl transferases, H3K27me3 compensates for H3K9me3 loss at interspersed and pericentromeric repeats (Peters et al., 2003). However, additional deletion of the Polycomb repressor complex 2 (PRC2) subunit EED can deregulate these repetitive sequences, indicating redundancy of repressive mechanisms (Walter, 2016). Proteomic analysis of ESCs indicates that 60% of histone H3 proteins are composed of H3K27me2/3 modifications (Peters et al., 2003). Collectively, these data suggest H3K27me3-based heterochromatinization provides a dynamic epigenetic mechanism that silences repeat sequence expression in response to alterations in other silencing mechanisms and likely contributes extensively on its own (Bulut-Karslioglu et al., 2014; Karimi et al., 2011; Liu et al., 2014). Despite this fundamental contribution to genome-wide repeat silencing, little is known about the mechanism of H3K27me3 deposition and expansion at repetitive sequences because investigation of Polycomb at non-unique genomic regions primarily concerns the regulation of neighboring genes (Bauer et al., 2015; Casa and Gabellini, 2012). Beyond ESCs, investigation of repetitive DNA silencing by PRC2 remains even less understood.

Dynamic response to various genomic alterations positions Polycomb as a robust barrier to reactivation of repeat sequences. Thus, disruption of genome stability through repeat sequence resurrection likely requires disruption of Polycomb-mediated heterochromatin. A surprising link among Polycomb, repetitive sequences, and cancer-initiating mechanisms may be the RB tumor suppressor protein (pRB). Although pRB is best known as a repressor of E2F transcription factors at cell-cycle genes, pRB family proteins also direct H3K27me3 to repress transcription during differentiation and stress (Blais et al., 2007; Bracken et al., 2007; Kareta et al., 2015; Kotake et al., 2007). In addition, RB-cell-cycle-independent interactions with chromatin (Avni et al., 2003; Wells et al., 2003) have been observed, but genome-wide analysis of pRB at repeat sequences is lacking (Coschi et al., 2014; Montoya-Durango et al., 2009). Thus, there is no evidence pRB-mediated regulation of H3K27me3 is sufficiently widespread to match the magnitude of H3K27me3 abundance and distribution at repeats.

In this study, we demonstrate that pRB and enhancer of zeste homolog 2 (EZH2) form a complex that directs H3K27me3 deposition at most repeat element types from simple sequence repeats and satellites to DNA transposons, long interspersed nuclear elements (LINEs), short interspersed nuclear elements (SINEs), and endogenous retroviruses. We report the generation of a strain of mice carrying a targeted point mutation, F832A (called $Rb1^S$), which is specifically defective for recruitment of EZH2 to repetitive sequences. In the absence of pRB recruitment, EZH2 no longer directs H3K27me3 to these elements, leading to dispersion or loss of heterochromatin. $Rb1^{S/S}$ fibroblasts and splenocytes express diverse repeat sequences, including tandem and interspersed elements, and aged $Rb1^{S/S}$ mice develop spontaneous lymphomas. Collectively, these data suggest that silencing of repetitive elements contributes to pRB's function as a tumor suppressor.

RESULTS

pRB Occupies Repetitive Genomic Sequences

To explore emerging chromatin regulatory functions beyond cell-cycle control, we compared pRB association with chromatin in arrested and proliferating mouse embryonic fibroblasts (MEFs). While noticeably reduced, pRB retains some chromatin binding in proliferating cells (Figure 1A). We sought to further investigate genome-wide distribution of pRB across growth conditions by chromatin immunoprecipitation-sequence analysis (ChIP-seq). We used a stringent sequence alignment approach that prohibited mismatches and randomized read assignments where more than one exact match existed to enhance potential alignments to repetitive regions (see Experimental Procedures and Bulut-Karslioglu et al., 2014). Analysis of distribution across broad genomic regions reveals a dramatic abundance of peaks in introns and intergenic locations (Figure 1B), with distribution proportions unaltered by proliferative status. This suggests that despite reduced pRB chromatin occupancy in proliferating cells, this pRB distribution pattern displays cell cycle independence at these regions. Comparison of enrichment at wild-type peak locations within promoters of $Rb1^{-/-}$ controls confirms a high degree of stringency in peak assignment (Figure 1C). Because an abundance of peaks localize to non-coding regions, we next annotated peaks on the basis of categories of repetitive sequences (Figure 1D). Analysis of peak distribution reveals pRB association with SINEs, long terminal repeat (LTR)-containing endogenous retroviruses (ERVs), LINEs, and simple repeat sequences, among others. Importantly, these surprising findings are mirrored in a meta-analysis of a recently published human pRB ChIP-seq study (Figures 1B and 1D) (Ferrari et al., 2014).

The RB protein is best known for its regulation of E2F-responsive cell-cycle genes, and our mapping of ChIP-seq reads detects these promoter occupancy events in mouse and human datasets (Figures 1E and 1F). Repeat occupying peaks are also found in neighboring regions of the same chromosomes (Figures 1G and 1H). Our analysis of peak distribution in murine cells demonstrates that at least two-thirds of pRB-occupying peaks map to repetitive sequences (Figures 1B and 1D). It is difficult to draw a similar conclusion in human data because many pRB peaks contain multiple repetitive elements in the same peak (Figure 1H). Collectively, these data indicate that pRB associates with diverse repetitive elements in mouse and human fibroblasts.

Loss of a CDK-Resistant pRB-E2F1 Interaction Disrupts Repeat Association

We previously identified a pRB-E2F1 interaction that confers reduced binding to consensus E2F sequence elements and resistance to disruption by cyclin dependent kinase (CDK) phosphorylation (Cecchini and Dick, 2011; Dick and Dyson, 2003). We sought to determine whether the properties of this interaction could underlie the cell-cycle-independent pRB occupancy observed in our ChIP-seq. We generated a targeted mutant mouse strain bearing an F832A substitution to disrupt the unique pRB-E2F1 interaction and named this allele $Rb1^S$ (Figures S1A–S1D, available online). $Rb1^{S/S}$ mice are indistinguishable from littermates (Figures S1E and S1F), and $Rb1^{S/S}$ cells exhibit
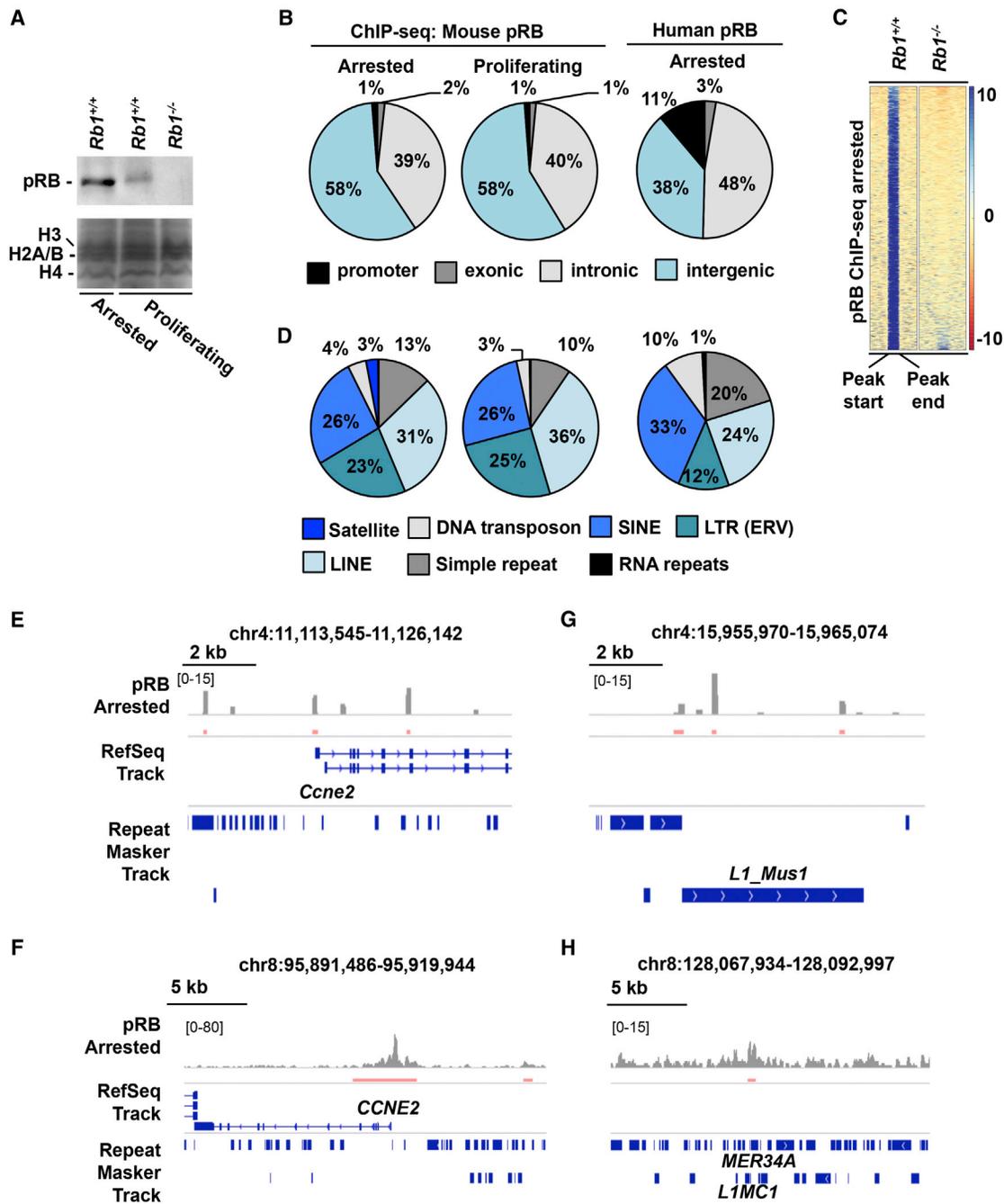
Figure 1. pRB Associates with Genomic Repeats in Murine and Human Fibroblasts

(A) pRB western blots of MEF chromatin fractions. Coomassie-stained histones indicate relative chromatin quantities.

(B) Overall genomic distribution of pRB ChIP-seq peaks per growth condition; n = 424,588 peaks and n = 77,809 peaks for mouse pRB in arrested and proliferating MEFs respectively; n = 71,511 peaks for human pRB in arrested IMR90 cells.

(C) Heatmaps display scaled pRB ChIP-seq read buildups at proximal promoter regions occupied by wild-type pRB peaks. Each row contains ± 1 kb of flanking sequence. The intensity scale indicates the read enrichment level.

(D) Percent distribution of pRB ChIP-seq peaks per repeat class; n = 321,892 peaks for mouse pRB arrested, n = 49,210 peaks for mouse pRB proliferating, and n = 99,186 peaks for human pRB arrested.

(E) Genome viewer tracks display mouse pRB ChIP-seq reads at *Ccne2*, with genomic coordinates above. Repeat Masker and RefSeq tracks are shown below. Red bars denote peaks.

(F) The analogous region of human *CCNE2* is shown and labeled akin to (D).

(G) Example of mouse pRB occupancy at a LINE-1 element 3′ of the *Ccne2* gene.

(H) Example of a human pRB peak 5′ of *CCNE2* that simultaneously overlaps multiple repeat elements.

ostensibly normal expression levels of pRB and RB family proteins (Figure 2A). pRB^S demonstrates a specific defect in binding the E2F1 coiled coil and marked box domain, without effects on E2F transactivation domain binding (Figures S2A–S2D). Consistent with this, cell-cycle regulation and E2F target gene expression are indistinguishable from wild-type controls (Figures S2E–S2G).

Western blots of chromatin fractions reveal diminished pRB^S association with chromatin under both proliferating and arrested conditions (Figure 2A). ChIP-qPCR was performed to assess pRB recruitment at the cell-cycle-responsive *Mcm3* promoter. In addition to *Rb1$^{S/S}$* cells, we utilized the previously characterized *Rb1^G* mutant that disrupts canonical pRB-E2F transcriptional control through R461E and K542E substitutions for comparison (Cecchini et al., 2014) (Figure 2B). Under arrested conditions, the pRB^S protein exhibits a similar association with the *Mcm3* transcriptional start site (TSS) as wild-type pRB, whereas the pRB^G mutant exhibits reduced occupancy. Under proliferating conditions, wild-type and pRB^S occupancy of the *Mcm3* promoter diminishes, which is consistent with CDK-dependent regulation of pRB-E2F interactions at this genomic location.

Given the retention of pRB^S at E2F cell-cycle targets, but the clear loss of chromatin association revealed by fractionation, we conducted ChIP-seq for pRB in *Rb1$^{S/S}$* cells to discover genomic locations that require this pRB-E2F1 interaction. Because pRB^S chromatin association was globally reduced in Figure 1A, we focused our analysis on wild-type locations lost in *Rb1$^{S/S}$* cells. Under both growth conditions, ChIP-seq in *Rb1$^{S/S}$* fibroblasts uncovers a dramatic loss of pRB enrichment at repetitive elements occupied by wild-type pRB that is equally evident by ChIP-qPCR (Figures 2C–2E). Comparison of read buildups at wild-type peak locations reveals that pRB^S localization is disrupted at the vast majority of elements in these repClass groups (Figure 2C). Quantitatively, greater than 80% of wild-type pRB peak intersections at repetitive elements are lost in *Rb1$^{S/S}$* chromatin under both growth conditions (Figure S3A).

In contrast to repetitive elements, the pRB^S enrichment profile at E2F cell-cycle genes parallels that of wild-type pRB (Figure S3B). Interestingly, pRB localizes extensively to repeat-containing regions within 1 kb of non-E2F target genes and pRB^S exhibits a loss of enrichment at these repeat-containing regions under both growth conditions (Figure S3C). ChIP-qPCR for pRB at major satellites, LTR-containing, and non-LTR retrotransposon repeat classes confirms diminished pRB^S occupancy at repetitive elements, whereas the pRB^G mutant parallels the cell-cycle-independent occupancy displayed by wild-type pRB at these elements (Figure 2D). Genome browser tracks show two examples of pRB peak loss in *Rb1$^{S/S}$* cells at fragments of LINE-1 elements (Figure 2E). Lastly, ChIP-qPCR detects E2F1 at these repetitive sequences, which is consistent with a model of E2F1 contributing to pRB localization at repeats (Figure S3D).

Collectively, these data indicate that disrupting pRB's CDK-resistant binding site for E2F1 prevents its localization to repetitive regions of the genome. Analysis of mutant forms of pRB with distinct defects for E2F interaction type across different growth conditions further supports the conclusion that pRB possesses a cell-cycle-independent mechanism for repeat occupancy

that is distinct from its transcriptional regulatory role during the G1-S phase transition.

pRB-Repeat Association Is Required to Silence Repetitive Sequence Expression

To investigate the functional role of repeat occupancy by pRB, we performed RNA-seq on arrested MEFs. Total RNA was depleted of rRNA prior to library construction, and reads were aligned to repeat indices and binned according to repeat classification and family. The number of reads in each category was normalized to the total number of aligned reads per sample. Columns display expression from three separate *Rb1$^{S/S}$* MEF preparations as a log$_2$ ratio normalized to the average of three wild-type samples (Figure 3A). *Rb1$^{S/S}$* MEFs exhibit increased expression of type I and type II transposable elements, satellites, and simple repeats in all three biological replicates. In two mutant samples, many families of LTR-containing repeats, DNA transposons, LINEs, and SINEs show widespread deregulation. Collectively, this demonstrates transcriptional misregulation of repeats that matches the repeat occupancy pattern of pRB. We note variability of expression in sample C5137_E3; however, broad differences between biological replicates are common to investigations of repeat sequence expression (Howard et al., 2008; Muotri et al., 2010; Wylie et al., 2016), and limited misregulation appears specific to this MEF preparation alone.

Representative elements from highly deregulated repeat classes were selected to further explore pRB-repeat regulation. Mapping sequence reads to instances of LINE-1, IAP, and major satellite sequences confirms increased read abundance across these elements (Figure 3B). Furthermore, elevated transcript levels from major satellites, LINE-1 elements, and intracisternal A particle (IAP) endogenous retroviruses are readily detectable in arrested and proliferating cultures of *Rb1$^{S/S}$* MEFs by qRT-PCR (Figures 3C and S4A). Elevated LINE-1 5′ UTR and IAP LTR-containing transcript levels are consistent with full-length element expression (Figures 3B and 3C). Again, we note that MEFs from embryo C5137_E3 are refractory to expression in three separate analyses of these cells. Microarray analysis was performed to compare the specificity of endogenous retroviral expression in *Rb1$^{S/S}$* cells with other structure-function mutants of pRB that disrupt binding to the E2F transactivation domain (*Rb1$^{G/G}$*) or to LXCXE-motif-containing proteins (*Rb1$^{L/L}$*). This analysis reveals increased expression of repeats specifically in the *Rb1$^{S/S}$* mutant and not the other genotypes (Figure 3D). Importantly, expression of canonical E2F target genes appears increased in only *Rb1$^{G/G}$* and *Rb1$^{L/L}$* cells (Figure S4B), further emphasizing the unique alteration in gene expression found in *Rb1$^{S/S}$* mutants.

These experiments demonstrate that pRB occupancy of repetitive sequences functionally contributes to their silencing because loss of binding correlates with increased expression of a wide array of repeats that are detectable using multiple expression-profiling methods. Curiously, many examples of pRB occupancy in Figures 1 and 2 are fragments of repetitive elements that may not be capable of autonomous expression. This suggests that this pRB-dependent silencing mechanism is broad and indiscriminate both in the elements that it silences and their potential for expression.
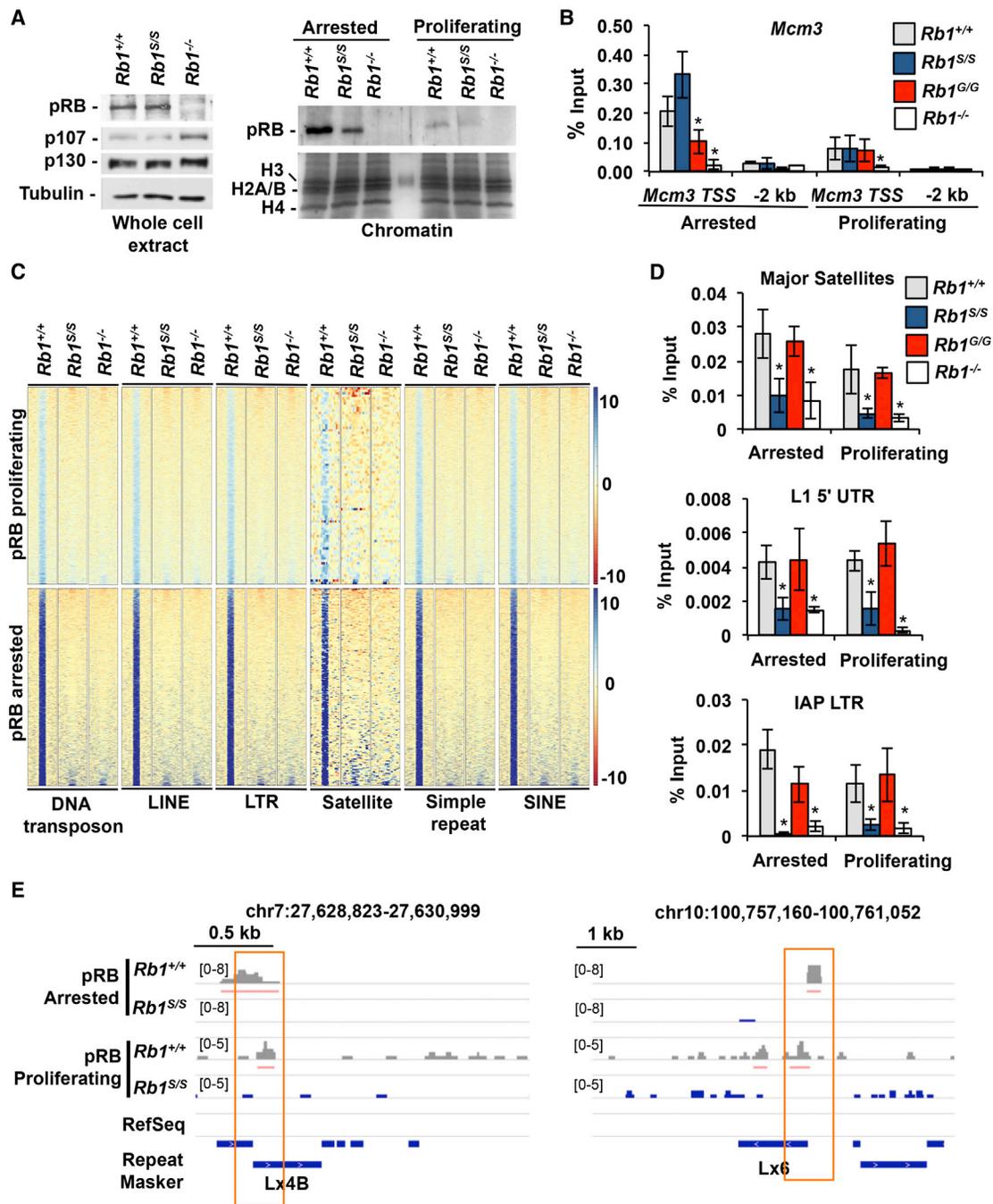
Figure 2. Cell-Cycle-Independent pRB-Repeat Association

(A) Western blots of whole-cell extracts display expression levels of wild-type and the F832A mutant ($Rb1^S$) pRB as well as p107 and p130. pRB western blot of chromatin fractions from arrested and proliferating cells. Coomassie-stained histones indicate loading.

(B) pRB ChIP-qPCR at the *Mcm3* TSS and 2 kb 5′ of *Mcm3*.

(C) Heatmaps of pRB ChIP-seq read enrichment per repClass. Each row represents one scaled wild-type peak location at an element within the repClass and includes ± 1 kb of flanking sequence. Intensity scale indicates magnitude of read enrichment.

(D) pRB ChIP-qPCR at the indicated repetitive elements.

(E) Representative genomic regions with pRB repeat association at LINE-1 fragments. Red bars denote peaks. For all graphs, error bars indicate one SD from the mean, and an asterisk represents a significant difference from wild type (p ≤ 0.05 by t test). See also Figures S1–S3.
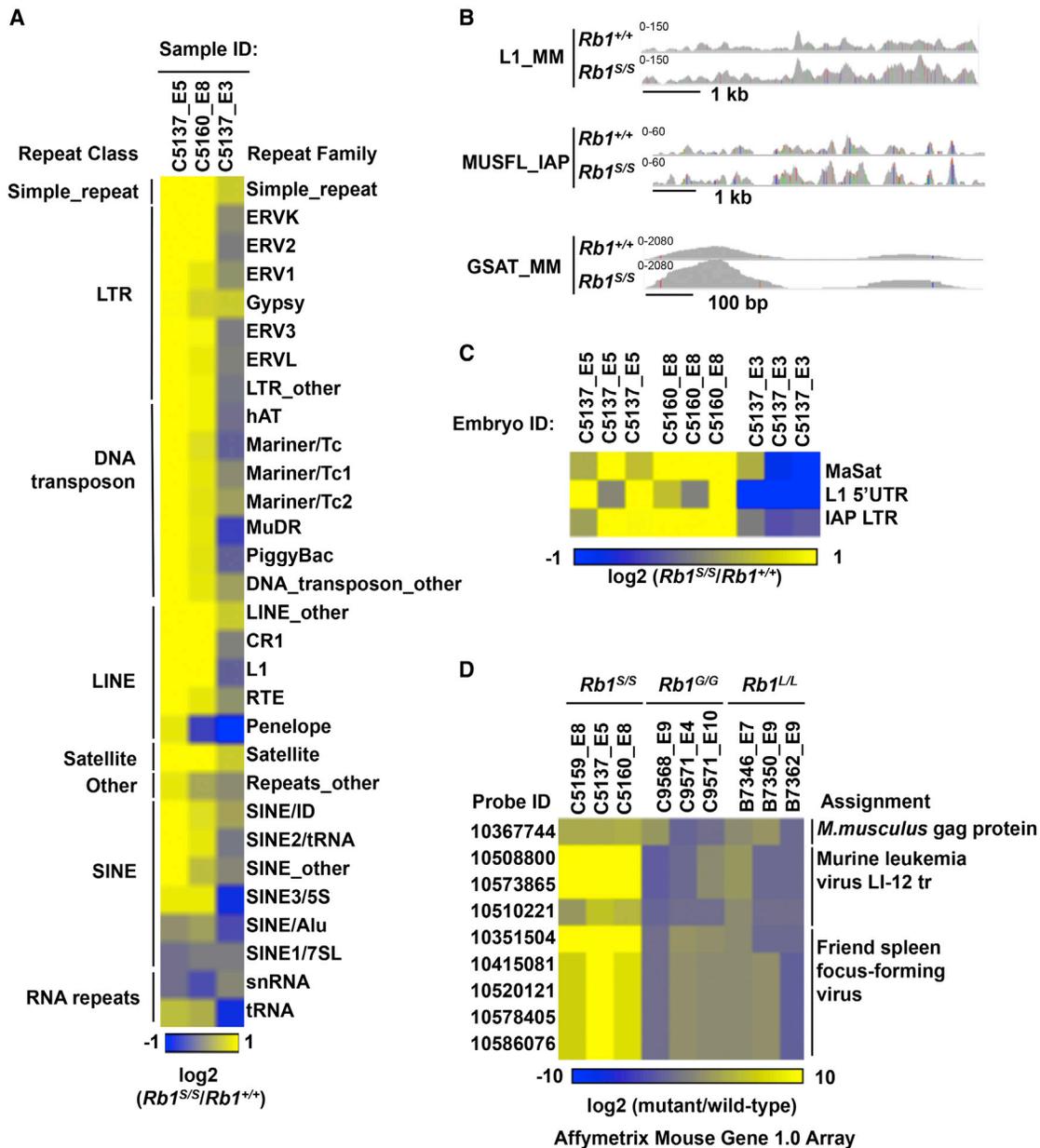
Figure 3. pRB Silences Repetitive Element Expression

(A) Heatmap of repeat expression from three *Rb1*^{S/S} MEF preparations relative to the average of three wild-type replicates. RNA-seq reads were aligned to repeat indices, binned according to repClass and repFamily, and normalized to the total number of aligned reads in the sample. Expression was quantified as a log₂ ratio relative to the average of three wild-type replicates.

(B) RNA-seq reads aligned to instances of LINE, IAP endogenous retrovirus, and major satellite repeats.

(C) qRT-PCR of the indicated repetitive elements in proliferating MEFs plotted as log2 of the ratio, with wild type using actin as an internal control. Each MEF pair was cultured independently three times and expression levels for each replicate are shown to illustrate variability in expression between culture and genotypes.

(D) Expression microarrays performed with RNA from arrested MEFs. Log2 values of mutant/wild type shown as a heatmap depict expression levels of endogenous retrovirus-detecting probe sets. See also Figure S4.

H3K27me3 Enrichment at Repetitive Sequences Is pRB Dependent

DNA methylation and histone modifications contribute to both redundant and non-redundant silencing of repetitive elements. The contribution of each was assessed in mutant fibroblasts. ChIP was used to detect histone tail modifications regulated by pRB and present at repetitive elements in ESCs. Although H4K20me3 and H3K9me3 enrichment remain unchanged at major satellites, LINEs, and LTR-containing endogenous retroviruses (Figures S5A and S5B), a prominent reduction of H3K27me3 appears evident in *Rb1*^{S/S} cells (Figure 4A). Beyond methylation, *Rb1*^{S/S} cells exhibit elevated H3K9Ac enrichment
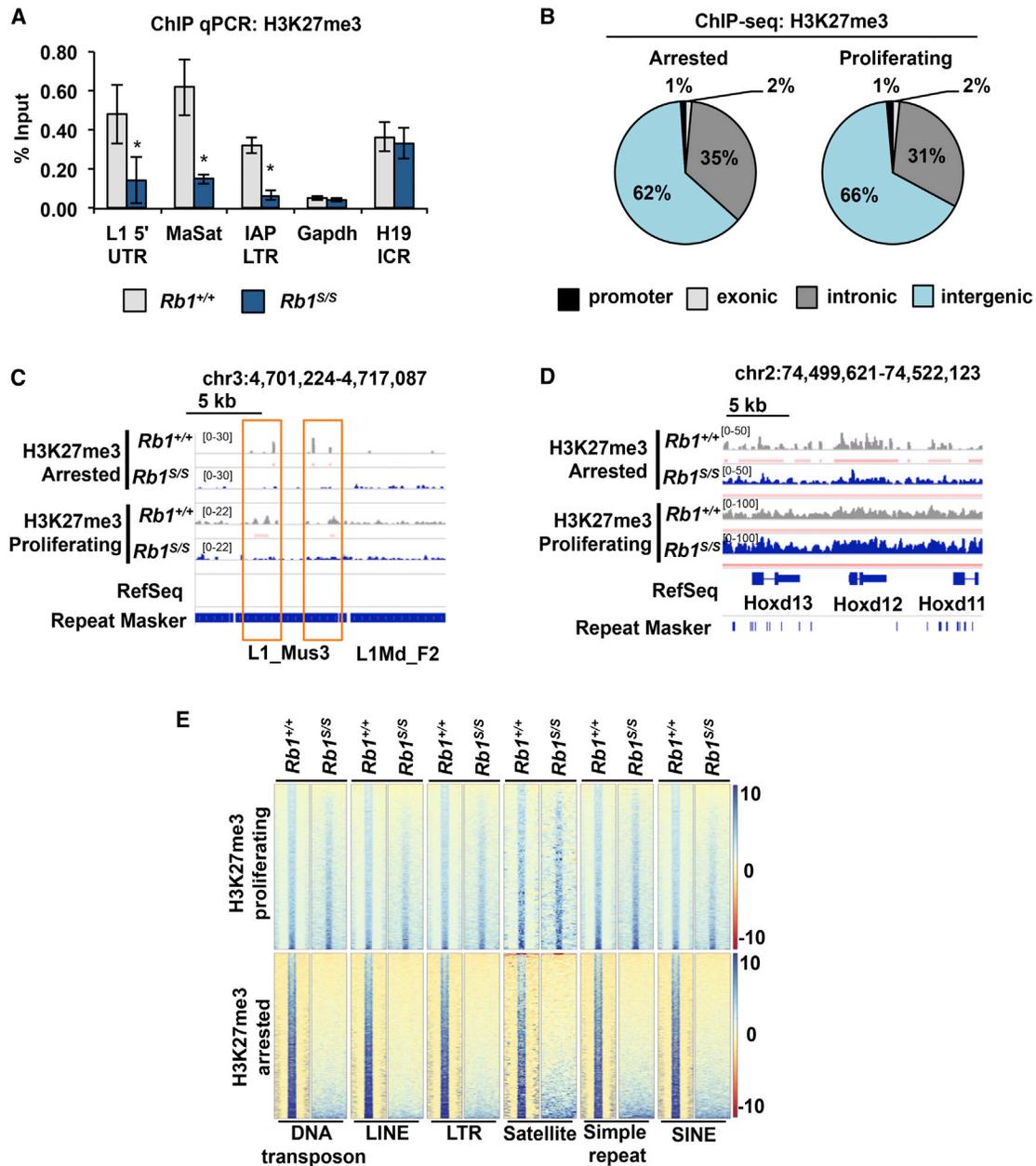
Figure 4. H3K27me3 Enrichment at Repetitive Elements Is pRB Dependent

(A) ChIP-qPCR for H3K27me3 in arrested MEFs. Error bars indicate one SD from the mean. An asterisk represents a significant difference from wild type (p ≤ 0.05 using a t test).

(B) Overall genomic distribution of H3K27me3 ChIP-seq peaks per growth condition; n = 656,342 peaks in arrested cells; n = 143,252 peaks in proliferating cells.

(C) Genome viewer tracks depict H3K27me3 read buildup at L1 elements (highlighted by red boxes), with genomic coordinates and scale above tracks.

(D) H3K27me3 distribution at a *Hox* gene cluster.

(E) Heatmaps of H3K27me3 read enrichment per repClass. Each row represents one scaled wild-type peak location at an element within the repClass and includes ± 1 kb of flanking region. Intensity scale indicates magnitude of read enrichment. See also Figures S5 and S6.

at these repetitive elements, and de-repression by Trichostatin A further suggests that histone de-acetylation functionally contributes to this regulation (Figure S5C). In contrast, *H19* and *Gapdh* maintain equivalent enrichment of these histone tail modifications between genotypes.

We performed ChIP-seq for H3K27me3 to expand upon the pRB dependence observed at repetitive elements by ChIP-qPCR. Similar to pRB, the vast majority of wild-type H3K27me3 peaks reside within intronic and intergenic regions, irrespective of proliferative status (Figure 4B). A number of

distinct effects of the *Rb1*[S/S] mutation on H3K27me3 distribution emerge from these data. H3K27me3 reductions are readily observed in sequence tracks over repeat-rich intergenic regions (Figure 4C). Many canonical genes regulated by H3K27me3, such as in *Hox* clusters, *Cdkn2a*, and *Sox2*, retain normal H3K27me3 enrichment in *Rb1*[S/S] MEFs (Figures 4D and S5D). Comparison of H3K27me3 read buildup at wild-type peak locations across repeat classes reveals diminished enrichment in *Rb1*[S/S] cells, particularly under arrested growth conditions (Figure 4E). However, some individual repeat elements disperse or broaden their H3K27me3 distribution, and this is more common in proliferating cells. Comparison of peak intersections at repetitive elements reveals that 75% of wild-type H3K27me3 peaks in repeat regions are lost in *Rb1*[S/S] cells across both growth conditions (Figure S5E). Retention of reads at many repeats in proliferating *Rb1*[S/S] cells (Figure 4E) at magnitudes below the threshold of peak calling suggests that H3K27me3 becomes dispersed, but not altogether lost, under proliferating conditions. Elevated repeat expression in proliferating *Rb1*[S/S] cells (Figure 3C) suggests this dispersion represents compromised silencing by H3K27me3.

These data demonstrate a broad mechanism of heterochromatinization among many distinct repeat element types. DNA methylation is perhaps the only other mechanism as indiscriminate in its repertoire of target sequences. Therefore, we investigated DNA methylation by bisulfite sequencing to determine if H3K27me3 and DNA methylation may be functionally related by pRB. Amplification of the same families of LINE-1 and IAP LTR viruses, as in Figures 2D and 3C, bears no obvious DNA methylation differences in *Rb1*[S/S] MEFs (Figures S6A and S6B). Following DNA methylation inhibition by 5-aza cytidine, repeat sequence expression increases in *Rb1*^{+/+}, but not *Rb1*[S/S], MEFs, suggesting that they are already de-repressed (Figure S6C).

Our data reveal a dramatic loss of H3K27me3 organization at repetitive sequences. H3K27me3 loss is similar in magnitude to loss of pRB at repeat sequences in *Rb1*[S/S] fibroblasts. Our data further suggest that DNA methylation alterations do not underlie widespread changes to heterochromatin in *Rb1*[S/S] cells. For this reason, we interpret our experiments to be indicative of a mechanism for silencing repetitive DNA sequences that acts in parallel to DNA methylation in primary fibroblasts.

pRB-Chromatin Association Is Required for EZH2 Recruitment to Repetitive Sequences

The polycomb repressor 2 complex (PRC2) contains the EZH2 histone methyltransferase that methylates H3K27 to establish the trimethylation mark. We explored whether pRB-dependent regulation of EZH2 might underlie epigenetic and transcriptional changes observed in *Rb1*[S/S] cells.

ChIP-seq was used to determine whether EZH2 association at repeat elements was affected in growth-arrested *Rb1*[S/S] cells. This analysis reveals that EZH2 also displays primarily intronic and intergenic distribution (Figure 5A). Across all repeat classes, wild-type locations of EZH2 enrichment diminish in *Rb1*[S/S] MEFs (Figure 5B), with more than 80% of wild-type peak intersections at repetitive elements lost in *Rb1*[S/S] fibroblasts (Figure S7A).

ChIP-qPCR confirms pRB-dependent EZH2 association with major satellites, LINEs, and endogenous retroviral sequences (Figure 5C). Because pRB and E2Fs control EZH2 expression (Bracken et al., 2003; Jung et al., 2010), we confirm EZH2 levels remain unchanged in *Rb1*[S/S] MEFs, and therefore do not mislead our investigation (Figure S7B). pRB-dependent EZH2 localization suggests regulation beyond transcriptional control of EZH2. Indeed, ChIP-reChIP indicates that EZH2 and pRB co-localize at LINE-1 and IAP LTRs, whereas association in *Rb1*[S/S] MEFs is comparable to background (Figure 5D). Co-immunoprecipitation demonstrates that both wild-type and pRB[S] bind EZH2 (Figure S7C). In addition, ChIP-reChIP reveals that E2F1 deficiency prevents pRB and EZH2 co-localization to LINE-1, IAP, and major satellite repeats (Figure S7D). Collectively, this suggests a model whereby pRB[S] can bind EZH2 but fails to localize to repetitive sequences because of its deficiency for binding E2F1, whereas wild-type pRB is capable of both EZH2 and E2F1 interactions, leading to H3K27me3 deposition at repetitive locations (Figure 5E).

Our data indicate that pRB, E2F1, and EZH2 are capable of forming a complex at repetitive genomic regions. However, although peak intersections between pRB and EZH2 at repetitive sequences in *Rb1*[S/S] cells assert a genetic requirement for pRB to recruit EZH2, they do not co-localize stoichiometrically (Figures S7E and S7F). This suggests that pRB and E2F1 may recruit EZH2 initially, but subsequent spreading of EZH2 and H3K27me3 may occur independent of pRB.

Rb1[S/S] Mice Succumb to Spontaneous Lymphoma

To determine where this repeat silencing mechanism is most relevant, we assessed repeat expression in tissues of adult mice using qRT-PCR (Figure 6A). For most tissues, expression varies between individuals, with no consistent trend relative to wild-type controls. However, four of eight *Rb1*[S/S] mice display elevated levels of all repeats tested in the spleen (F241, F242, F248, and F307), whereas only one of eight wild-type mice expresses repeats in this tissue (F233). This suggests that pRB-dependent silencing may be most relevant in the spleen. However, a survey of major tissues in these mice, including the spleen, reveals no obvious histological differences. Given that expression of repetitive sequences stimulates an immune response to eliminate these cells, we searched for evidence of interferon activation. Figure 6B shows qRT-PCR analysis of *Ifn-α* and *Ifn-β* expression in splenocytes. Again, expression varies among individuals, but we note that two *Rb1*[S/S] mice display high-level expression of both (F296 and F307), further suggesting that *Rb1*[S/S] mice respond to abnormal repeat expression in their splenocytes. Conversely, this magnitude of interferon response is largely absent from wild-type mice. Because normal mammalian immune function seeks to eliminate repeat misexpressing cells, we further sought evidence of altered repression by investigating H3K27me3 deposition at repetitive sequences in splenocytes. ChIP-qPCR assays demonstrate that H3K27me3 is reduced at IAP ERVs, LINE-1 elements, and major satellites, but H3 levels remain comparable between genotypes (Figure 6C). These experiments suggest that H3K27me3 is altered in chromatin from *Rb1*[S/S] splenocytes and that repeats can be misexpressed, but these cells are likely
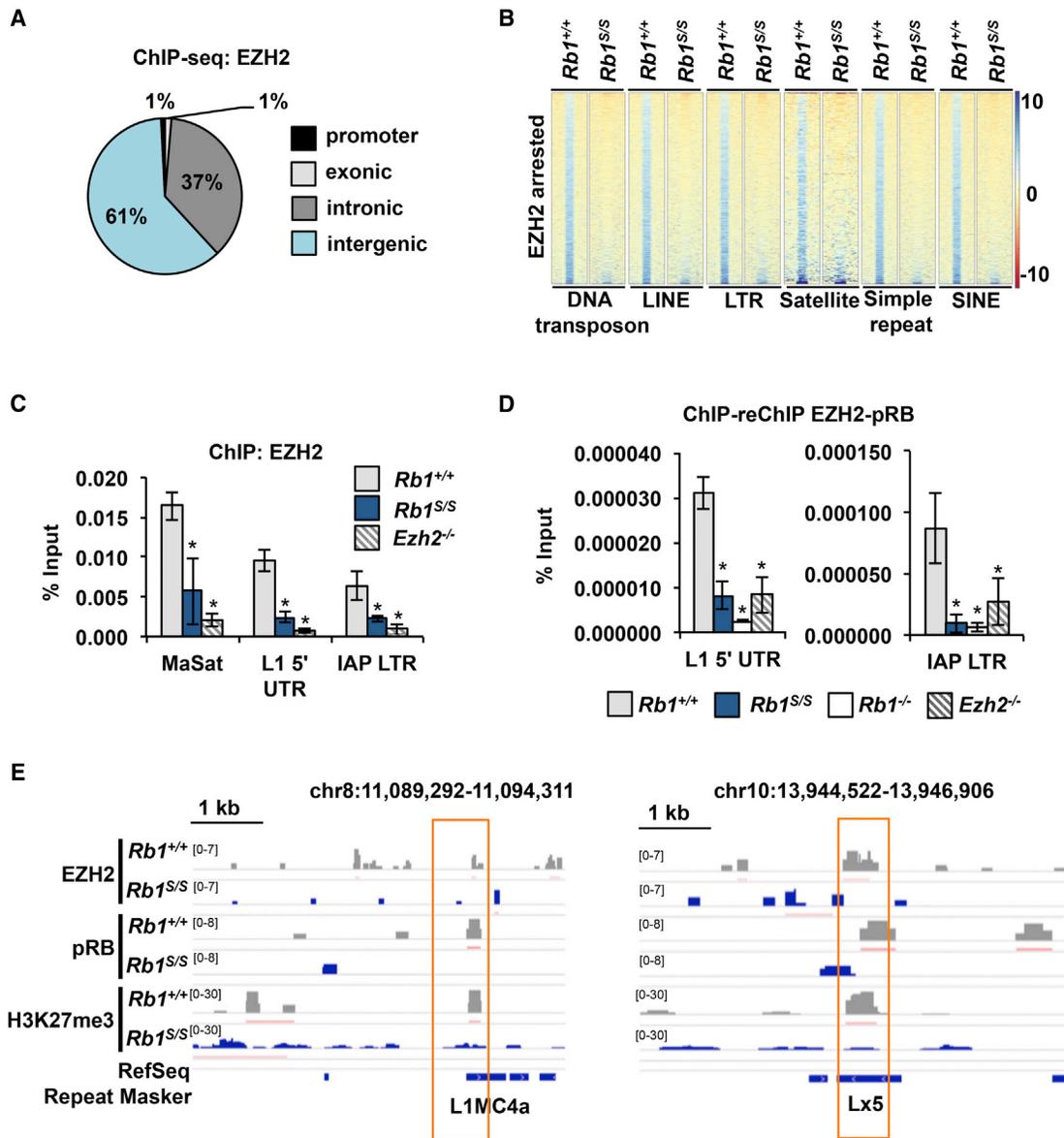
Figure 5. pRB-Chromatin Association Mediates EZH2 Recruitment to Repetitive DNA

(A) Overall genomic distribution of EZH2 ChIP-seq peaks in arrested wild-type MEFs; n = 840,543 peaks.

(B) Heatmaps of EZH2 read enrichment per repClass. Each row represents one scaled wild-type peak location at an element within the repClass that includes ± 1 kb of flanking region. Intensity scale indicates level of read enrichment.

(C) EZH2 ChIP-qPCR at repeats.

(D) EZH2-pRB ChIP-reChIP at repeats, with genetic knockouts as controls.

(E) Two genomic regions depict ChIP-seq tracks for EZH2, pRB, and H3K27me3 in arrested MEFs, with genomic coordinates and scale above tracks. Red boxes highlight peak overlaps across datasets. For all graphs, error bars indicate one SD from the mean. An asterisk represents a significant difference from wild type (p ≤ 0.05 using a t test). See also Figure S7.

unable to accumulate in young adult mice with a functional immune system.

To determine the long-term consequences of the $Rb1^S$ mutation, we generated cohorts of $Rb1^{S/S}$ mutant mice and wild-type siblings to monitor over the course of their lifetime for the manifestation of pathology. Mutant mice exhibit a significantly reduced tumor-free survival, with a median lifespan of 576 days (Figure 7A). Necropsy and histopathological analysis reveals that the majority of mice succumb to lymphomas, particularly in the spleen and mesenteric lymph node (Figure 7B). Examples of lesions evident upon necropsy are shown in Figure 7C as well as the normal abdominal cavity of an unaffected wild-type mouse at 2 years of age. The corresponding histology for each example is shown (Figure 7D). In addition,
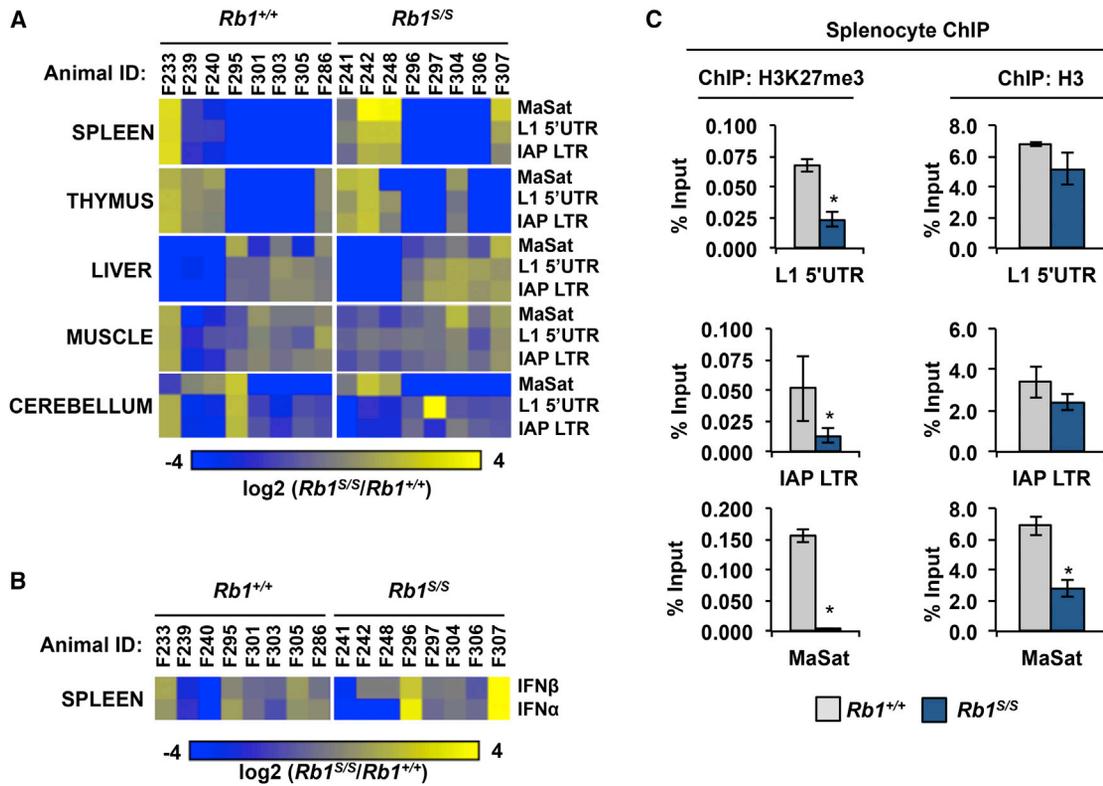
Figure 6. Altered Chromatin and Repeat Expression in *Rb1*^{S/S} Splenocytes

(A) Heatmap of repeat element expression per tissue of 6- to 8-week-old mice quantified by qRT-PCR. Log2 ratio of expression is displayed relative to the average of all wild-type measurements for a given element in each tissue.

(B) Heatmap of interferon gene expression in splenocytes from the same mice.

(C) H3K27me3 and H3 ChIP-qPCR from freshly harvested splenocytes of 6-week-old mice. Error bars indicate one SD from the mean (n = 3; an asterisk indicates $p < 0.05$, t test).

qRT-PCR of RNA derived from these tumor samples indicates that diverse repetitive sequences are expressed in these malignancies (Figure S7G). This suggests that pRB's ability to form complexes with E2F1 at repetitive sequences and establish H3K27me3-dependent silencing is highly relevant to its tumor suppressive functions.

Collectively, our work suggests a model in which pRB recruits EZH2 to repeat sequences, where it catalyzes H3K27me3 to silence expression, and a point mutation in pRB that blocks localization to these sequences prevents recruitment of EZH2 and causes dispersion of H3K27me3. Endogenously, this mechanism is important in splenocytes, where deregulated expression of repeats is most detectable, and these cells eventually give rise to lymphomas in older *Rb1*^{S/S} mice.

DISCUSSION

Our data reveal a mechanism, in which pRB and EZH2 cooperate to establish H3K27me3, which silences expression of genomic repeat sequences. This mechanism is largely indiscriminate because it silences tandem repeats in addition to retrotransposons. These characteristics indicate that pRB-EZH2-dependent silencing of repeats plays a broad but previously unappreciated role in genome organization.

Investigation of Polycomb-based repeat regulation by H3K27me3 in mammals primarily concerns critical steps of early embryonic development (Leeb et al., 2010; Macfarlan et al., 2012). Misregulation typically manifests in defects that prevent embryonic development before implantation (Leeb et al., 2010; Macfarlan et al., 2012) or that have overt consequences in adult mice (Li et al., 2015). Lack of developmental impediments in *Rb1*^{S/S} mice and retention of H3K27me3 at developmentally regulated loci, such as *Hox* genes and *Sox2*, suggests the pRB-EZH2 complex must be recruited to repeats through a mechanism that is distinct from previous studies, or this pRB-dependent mechanism is not functional in cells during early development.

Comprehensive understanding of the Polycomb function requires detailed elucidation of chromatin recruitment mechanisms (Bauer et al., 2015; Casa and Gabellini, 2012). Previous studies demonstrate that non-coding transcripts can target Polycomb repressor complexes to specific loci, as observed upon X chromosome inactivation (Blackledge et al., 2015). Based on the co-immunoprecipitation of pRB and EZH2 and their co-occupancy of repeats by ChIP-reChIP, it is likely that pRB directly recruits EZH2 to repeats. Diminished pRB binding to repeats in *Rb1*^{S/S} cells results in loss of EZH2 and H3K27me3 peaks, but our data also suggest that EZH2 may
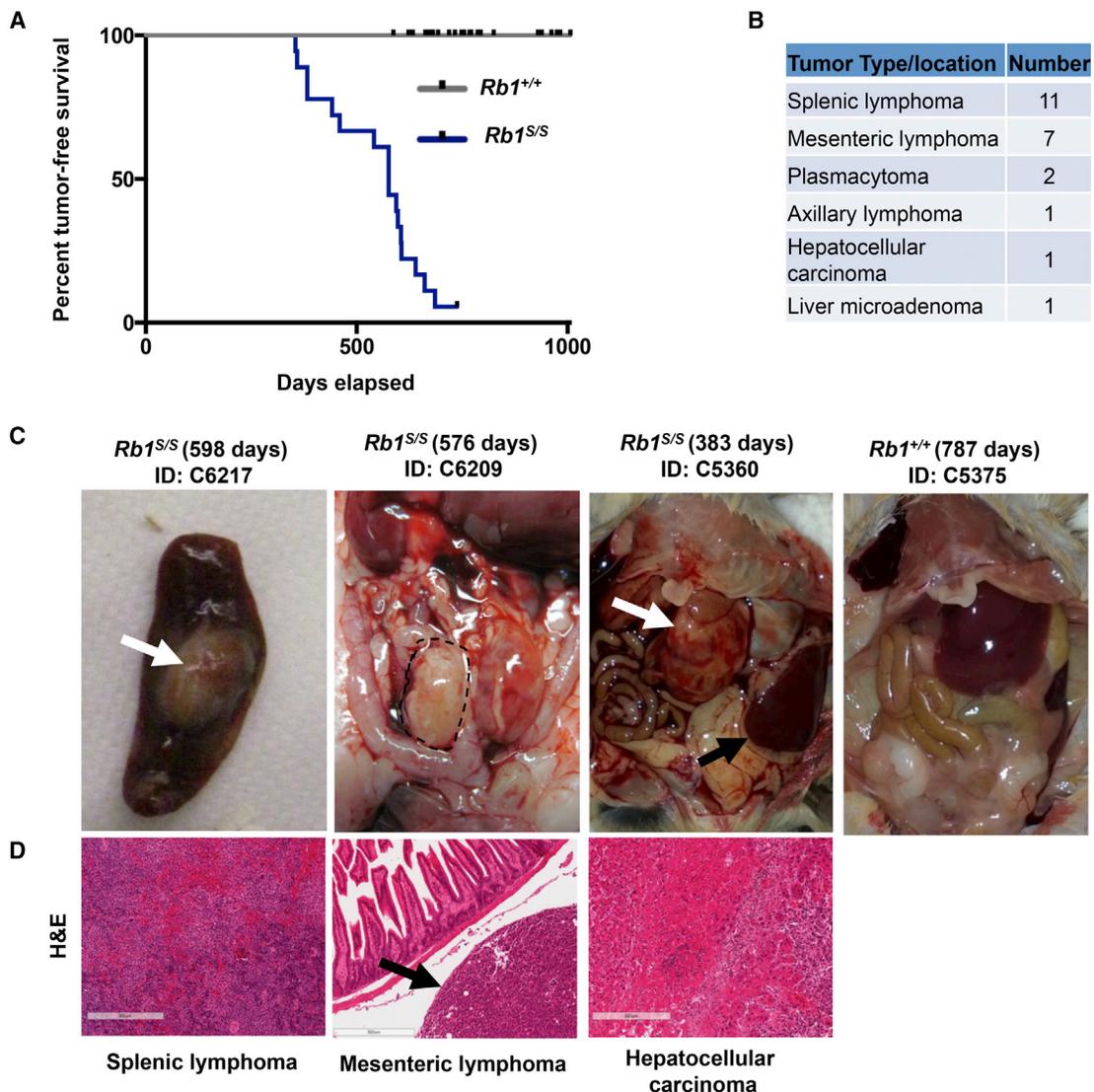
Figure 7. Aged *Rb1*^{S/S} Mice Are Tumor Prone

(A) Kaplan-Meier plot of tumor-free survival for cohorts of mice aged until animal protocol endpoint. Tick marks indicate mice necropsied at intermediate ages. Mutant mice are significantly more cancer prone than wild-type mice (log rank test, $p < 0.05$).

(B) Anatomical location and cancer type listed by frequency of occurrence.

(C) Peritoneal cavity images upon necropsy. A white arrow indicates an abnormal mass in the spleen of mouse C6217. A dashed line highlights the mesenteric lymph node of mouse C6209. A white arrow indicates an abnormal liver, and a black arrow indicates a normal lobe in mouse C5360.

(D) H&E staining of tissue sections from the abnormality indicated in the mutant animals above. A black arrow indicates the lymph node in mouse C6209. The scale bars represent 300 μm.

not stably associate with pRB at all of these locations and may spread H3K27me3 heterochromatin without it.

Beyond non-coding RNAs, sequence specific transcription factors can recruit Polycomb to specific genomic locations to initiate such nucleation and spreading (Bauer et al., 2015; Casa and Gabellini, 2012). Our study indicates that E2F1 can fulfill this role, and although some repeats contain consensus E2F elements (Montoya-Durango et al., 2009), E2F1 site selection appears increasingly diverse in the post-genomic era (Bieda et al., 2006; Biswas and Johnson, 2012). Our initial identification of pRB's unique interaction with E2F1 was based on

the inability of this complex to recognize a consensus E2F promoter element (Dick and Dyson, 2003). Major satellite repeats exemplify this in vivo where GC-rich consensus E2F elements are missing, but pRB and E2F1 bind cooperatively, such that E2F1 binding is greatly diminished without pRB (Coschi et al., 2014). Therefore, pRB-E2F1 interactions underlie recruitment of Polycomb to repeats; however, a recognition mechanism for E2F1 at the variety of repeat sequences identified remains unclear and is highly reminiscent of searches for Polycomb response elements in mammalian gene promoters (Bauer et al., 2015).

The cancer susceptibility of $Rb1^{S/S}$ mice suggests a role for pRB-EZH2 in genome maintenance and tumor suppression. This begs the question of how this mechanism functions endogenously, particularly because upregulation of repeat sequences in the spleen appeared quite variable. We note that elevated repetitive elements are detectable in splenocytes from cancer-prone $Tlr3$, $Tlr7$, and $Tlr9$ triple-deficient mice (Yu et al., 2012), even though chromatin-dependent repression mechanisms are wild-type. This implies that immune surveillance acts to eliminate wild-type cells that sporadically express repetitive elements on an ongoing basis, even if their repressive mechanisms are normal. This may explain the high degree of variability in repeat expression found in cells deficient for DNA-methylation- or histone-methylation-dependent repressive mechanisms (Howard et al., 2008; Muotri et al., 2010; Wylie et al., 2016). In this way, splenocytes of $Rb1^{S/S}$ mice may be poised to over-express repeats but are eliminated by immune detection mechanisms, preventing their accumulation and consistent detection of repeat expression.

It is difficult to conclude that repeat expression alone causes cancer in $Rb1^{S/S}$ mice. However, there are a number of reasons to expect that a pRB-E2F1-EZH2 complex has cancer-relevant properties. First, the preference for lymphomas and age of onset in $Rb1^{S/S}$ mice phenotypically parallels $E2f1^{-/-}$ mice (Yamasaki et al., 1996). Missense alleles in human $RB1$ are rare, so it is not surprising that the $Rb1^{S}$ allele is absent from cancer genome datasets. However, a low penetrance $RB1$ family has been reported to possess exon 24 and 25 deletions (Bremner et al., 1997) that eliminate pRB's unique binding domain for E2F1 (Cecchini and Dick, 2011; Julian et al., 2008). Similarly, multiple instances of D295 substitutions in DP1 (Munro et al., 2014) indicate that the unique contact point for E2F1/DP1 with pRB is directly targeted in human cancers. Lastly, other $Rb1$-targeted strains that compromise E2F transcriptional control at canonical cell-cycle target genes, such as $Rb1^{G/G}$ (Cecchini et al., 2014), or that are prone to unstable genomes related to defective chromatin condensation, as in $Rb1^{L/L}$ and $Rb1^{NF/NF}$ mice (Coschi et al., 2010; Vormer et al., 2014), are not spontaneously cancer prone. Because only $Rb1^{S/S}$ cells misexpress repeat sequences among these genotypes, and repeat expression is most pronounced in the cancer-prone tissue of $Rb1^{S/S}$ mice, these data point to a very strong correlation between defective pRB-EZH2 repeat suppression and cancer incidence.

Likely, the most significant implication for our work is the relationship between $RB1$ status and the effects of EZH2 inhibitors. We anticipate that EZH2 inhibitors will cause widespread de-repression of repetitive sequences in pRB-positive cancers, as reported for inhibitors of DNA methylation (Chiappinelli et al., 2015; Roulois et al., 2015), and this may offer a pathway to sensitize tumors to immunotherapy. By extension, EZH2 inhibitors may have activity as anti-viral agents because they may awaken latent viral genomes. This manuscript reveals an exciting connection between a canonical tumor suppressor and heterochromatin formation that further supports repetitive element silencing as a cancer-relevant process.

EXPERIMENTAL PROCEDURES

Cell Culture and Mice
MEFs were generated from E13.5 embryos and cultured as previously described (Coschi et al., 2014). Cells were typically arrested by serum starvation. All mice were handled according to CCAC standards.

Chromatin Immunoprecipitation
Briefly, cross-linked chromatin sonicated to ≤400 bp was normalized between experimental groups and pre-cleared with protein G Dynabeads, and ChIP antibodies were added to immunoprecipitate proteins. Cross-links were reversed at 65°C, and samples were treated with RNase and proteinase K. DNA was isolated for qPCR or library preparation, followed by single-end sequencing using Illumina HiSeq2500. See Tables S1 and S2 for ChIP-qPCR primers. Further details of ChIP-reChIP and ChIP-seq are available in the Supplemental Experimental Procedures.

RNA Expression
Total RNA isolated with Trizol was DNaseI-treated and reverse transcribed using random primers and Superscript III reverse transcriptase (Invitrogen). qRT-PCR was performed using iQ SYBR green Super Mix (Bio-Rad). See Supplemental Information for primer sequences. Expression microarray experiments can be found in GEO: GSE85640.

Analysis of ChIP-Seq and RNA-Seq Experiments
Sequence reads were mapped to the mm9 genome assembly, without allowing mismatches, as previously reported (Bulut-Karslioglu et al., 2014). Reads with more than one exact match were randomly assigned among these locations. RNA-seq reads were mapped to a custom repeat index (Day et al., 2010), assigning reads to their best match and allowing up to two sequence mismatches. See Supplemental Information for computational analysis details.

ACCESSION NUMBERS

The accession number for the sequence data reported in this paper is GEO: GSE85640.

SUPPLEMENTAL INFORMATION

Supplemental information includes Supplemental Experimental Procedures, seven figures, and two tables and can be found with this article online at http://dx.doi.org/10.1016/j.molcel.2016.10.021.

AUTHOR CONTRIBUTIONS

ACKNOWLEDGMENTS

REFERENCES

Avni, D., Yang, H., Martelli, F., Hofmann, F., ElShamy, W.M., Ganesan, S., Scully, R., and Livingston, D.M. (2003). Active localization of the retinoblastoma protein in chromatin and its response to S phase DNA damage. Mol. Cell *12*, 735–746.

Bauer, M., Trupke, J., and Ringrose, L. (2015). The quest for mammalian Polycomb response elements: are we there yet? Chromosoma *125*, 471–496.

Bersani, F., Lee, E., Kharchenko, P.V., Xu, A.W., Liu, M., Xega, K., MacKenzie, O.C., Brannigan, B.W., Wittner, B.S., Jung, H., et al. (2015). Pericentromeric satellite repeat expansions through RNA-derived DNA intermediates in cancer. Proc. Natl. Acad. Sci. USA *112*, 15148–15153.

Bieda, M., Xu, X., Singer, M.A., Green, R., and Farnham, P.J. (2006). Unbiased location analysis of E2F1-binding sites suggests a widespread role for E2F1 in the human genome. Genome Res. *16*, 595–605.

Biswas, A.K., and Johnson, D.G. (2012). Transcriptional and nontranscriptional functions of E2F1 in response to DNA damage. Cancer Res. *72*, 13–17.

Blackledge, N.P., Rose, N.R., and Klose, R.J. (2015). Targeting Polycomb systems to regulate gene expression: modifications to a complex story. Nat. Rev. Mol. Cell Biol. *16*, 643–649.

Blais, A., van Oevelen, C.J., Margueron, R., Acosta-Alvear, D., and Dynlacht, B.D. (2007). Retinoblastoma tumor suppressor protein-dependent methylation of histone H3 lysine 27 is associated with irreversible cell cycle exit. J. Cell Biol. *179*, 1399–1412.

Bracken, A.P., Pasini, D., Capra, M., Prosperini, E., Colli, E., and Helin, K. (2003). EZH2 is downstream of the pRB-E2F pathway, essential for proliferation and amplified in cancer. EMBO J. *22*, 5323–5335.

Bracken, A.P., Kleine-Kohlbrecher, D., Dietrich, N., Pasini, D., Gargiulo, G., Beekman, C., Theilgaard-Mönch, K., Minucci, S., Porse, B.T., Marine, J.C., et al. (2007). The Polycomb group proteins bind throughout the INK4A-ARF locus and are disassociated in senescent cells. Genes Dev. *21*, 525–530.

Bremner, R., Du, D.C., Connolly-Wilson, M.J., Bridge, P., Ahmad, K.F., Mostachfi, H., Rushlow, D., Dunn, J.M., and Gallie, B.L. (1997). Deletion of RB exons 24 and 25 causes low-penetrance retinoblastoma. Am. J. Hum. Genet. *61*, 556–570.

Bulut-Karslioglu, A., De La Rosa-Velázquez, I.A., Ramirez, F., Barenboim, M., Onishi-Seebacher, M., Arand, J., Galán, C., Winter, G.E., Engist, B., Gerle, B., et al. (2014). Suv39h-dependent H3K9me3 marks intact retrotransposons and silences LINE elements in mouse embryonic stem cells. Mol. Cell *55*, 277–290.

Casa, V., and Gabellini, D. (2012). A repetitive elements perspective in Polycomb epigenetics. Front. Genet. *3*, 199.

Cecchini, M.J., and Dick, F.A. (2011). The biochemical basis of CDK phosphorylation-independent regulation of E2F1 by the retinoblastoma protein. Biochem. J. *434*, 297–308.

Cecchini, M.J., Thwaites, M.J., Talluri, S., MacDonald, J.I., Passos, D.T., Chong, J.L., Cantalupo, P., Stafford, P.M., Sáenz-Robles, M.T., Francis, S.M., et al. (2014). A retinoblastoma allele that is mutated at its common E2F interaction site inhibits cell proliferation in gene-targeted mice. Mol. Cell. Biol. *34*, 2029–2045.

Chiappinelli, K.B., Strissel, P.L., Desrichard, A., Li, H., Henke, C., Akman, B., Hein, A., Rote, N.S., Cope, L.M., Snyder, A., et al. (2015). Inhibiting DNA methylation causes an interferon response in cancer via dsRNA including endogenous retroviruses. Cell *162*, 974–986.

Coschi, C.H., Martens, A.L., Ritchie, K., Francis, S.M., Chakrabarti, S., Berube, N.G., and Dick, F.A. (2010). Mitotic chromosome condensation mediated by the retinoblastoma protein is tumor-suppressive. Genes Dev. *24*, 1351–1363.

Coschi, C.H., Ishak, C.A., Gallo, D., Marshall, A., Talluri, S., Wang, J., Cecchini, M.J., Martens, A.L., Percy, V., Welch, I., et al. (2014). Haploinsufficiency of an RB-E2F1-Condensin II complex leads to aberrant replication and aneuploidy. Cancer Discov. *4*, 840–853.

Day, D.S., Luquette, L.J., Park, P.J., and Kharchenko, P.V. (2010). Estimating enrichment of repetitive elements from high-throughput sequence data. Genome Biol. *11*, R69.

Dick, F.A., and Dyson, N. (2003). pRB contains an E2F1-specific binding domain that allows E2F1-induced apoptosis to be regulated separately from other E2F activities. Mol. Cell *12*, 639–649.

Ferrari, R., Gou, D., Jawdekar, G., Johnson, S.A., Nava, M., Su, T., Yousef, A.F., Zemke, N.R., Pellegrini, M., Kurdistani, S.K., et al. (2014). Adenovirus small E1A employs the lysine acetylases p300/CBP and tumor suppressor Rb to repress select host genes and promote productive virus infection. Cell Host Microbe *16*, 663–676.

Helman, E., Lawrence, M.S., Stewart, C., Sougnez, C., Getz, G., and Meyerson, M. (2014). Somatic retrotransposition in human cancer revealed by whole-genome and exome sequencing. Genome Res. *24*, 1053–1063.

Howard, G., Eiges, R., Gaudet, F., Jaenisch, R., and Eden, A. (2008). Activation and transposition of endogenous retroviral elements in hypomethylation induced tumors in mice. Oncogene *27*, 404–408.

Iskow, R.C., McCabe, M.T., Mills, R.E., Torene, S., Pittard, W.S., Neuwald, A.F., Van Meir, E.G., Vertino, P.M., and Devine, S.E. (2010). Natural mutagenesis of human genomes by endogenous retrotransposons. Cell *141*, 1253–1261.

Julian, L.M., Palander, O., Seifried, L.A., Foster, J.E., and Dick, F.A. (2008). Characterization of an E2F1-specific binding domain in pRB and its implications for apoptotic regulation. Oncogene *27*, 1572–1579.

Jung, J.W., Lee, S., Seo, M.S., Park, S.B., Kurtz, A., Kang, S.K., and Kang, K.S. (2010). Histone deacetylase controls adult stem cell aging by balancing the expression of polycomb genes and jumonji domain containing 3. Cell. Mol. Life Sci. *67*, 1165–1176.

Kareta, M.S., Gorges, L.L., Hafeez, S., Benayoun, B.A., Marro, S., Zmoos, A.F., Cecchini, M.J., Spacek, D., Batista, L.F., O'Brien, M., et al. (2015). Inhibition of pluripotency networks by the Rb tumor suppressor restricts reprogramming and tumorigenesis. Cell Stem Cell *16*, 39–50.

Karimi, M.M., Goyal, P., Maksakova, I.A., Bilenky, M., Leung, D., Tang, J.X., Shinkai, Y., Mager, D.L., Jones, S., Hirst, M., et al. (2011). DNA methylation and SETDB1/H3K9me3 regulate predominantly distinct sets of genes, retroelements, and chimeric transcripts in mESCs. Cell Stem Cell *8*, 676–687.

Kotake, Y., Cao, R., Viatour, P., Sage, J., Zhang, Y., and Xiong, Y. (2007). pRB family proteins are required for H3K27 trimethylation and Polycomb repression complexes binding to and silencing p16INK4alpha tumor suppressor gene. Genes Dev. *21*, 49–54.

Lamprecht, B., Walter, K., Kreher, S., Kumar, R., Hummel, M., Lenze, D., Kochert, K., Bouhlel, M.A., Richter, J., Soler, E., et al. (2010). Derepression of an endogenous long terminal repeat activates the CSF1R proto-oncogene in human lymphoma. Nat. Med. *16*, 571–579.

Lander, E.S., Linton, L.M., Birren, B., Nusbaum, C., Zody, M.C., Baldwin, J., Devon, K., Dewar, K., Doyle, M., FitzHugh, W., et al.; International Human Genome Sequencing Consortium (2001). Initial sequencing and analysis of the human genome. Nature *409*, 860–921.

Lee, E., Iskow, R., Yang, L., Gokcumen, O., Haseley, P., Luquette, L.J., 3rd, Lohr, J.G., Harris, C.C., Ding, L., Wilson, R.K., et al.; Cancer Genome Atlas Research Network (2012). Landscape of somatic retrotransposition in human cancers. Science *337*, 967–971.

Leeb, M., Pasini, D., Novatchkova, M., Jaritz, M., Helin, K., and Wutz, A. (2010). Polycomb complexes act redundantly to repress genomic repeats and genes. Genes Dev. *24*, 265–276.

Leonova, K.I., Brodsky, L., Lipchick, B., Pal, M., Novototskaya, L., Chenchik, A.A., Sen, G.C., Komarova, E.A., and Gudkov, A.V. (2013). p53 cooperates with DNA methylation and a suicidal interferon response to maintain epigenetic silencing of repeats and noncoding RNAs. Proc. Natl. Acad. Sci. USA *110*, E89–E98.

Leung, D.C., and Lorincz, M.C. (2012). Silencing of endogenous retroviruses: when and why do histone marks predominate? Trends Biochem. Sci. *37*, 127–133.

Levin, H.L., and Moran, J.V. (2011). Dynamic interactions between transposable elements and their hosts. Nat. Rev. Genet. *12*, 615–627.

Li, W., Lee, M.H., Henderson, L., Tyagi, R., Bachani, M., Steiner, J., Campanac, E., Hoffman, D.A., von Geldern, G., Johnson, K., et al. (2015). Human endogenous retrovirus-K contributes to motor neuron disease. Sci. Transl. Med. *7*, 307ra153.

Liu, S., Brind'Amour, J., Karimi, M.M., Shirane, K., Bogutz, A., Lefebvre, L., Sasaki, H., Shinkai, Y., and Lorincz, M.C. (2014). Setdb1 is required for germline development and silencing of H3K9me3-marked endogenous retroviruses in primordial germ cells. Genes Dev. *28*, 2041–2055.

Lock, F.E., Rebollo, R., Miceli-Royer, K., Gagnier, L., Kuah, S., Babaian, A., Sistiaga-Poveda, M., Lai, C.B., Nemirovsky, O., Serrano, I., et al. (2014). Distinct isoform of FABP7 revealed by screening for retroelement-activated genes in diffuse large B-cell lymphoma. Proc. Natl. Acad. Sci. USA *111*, E3534–E3543.

Macfarlan, T.S., Gifford, W.D., Driscoll, S., Lettieri, K., Rowe, H.M., Bonanomi, D., Firth, A., Singer, O., Trono, D., and Pfaff, S.L. (2012). Embryonic stem cell potency fluctuates with endogenous retrovirus activity. Nature *487*, 57–63.

Mager, D.L., and Stoye, J.P. (2015). Mammalian endogenous retroviruses. Microbiol. Spectr. *3*, MDNA3-0009-2014.

Montoya-Durango, D.E., Liu, Y., Teneng, I., Kalbfleisch, T., Lacy, M.E., Steffen, M.C., and Ramos, K.S. (2009). Epigenetic control of mammalian LINE-1 retrotransposon by retinoblastoma proteins. Mutat. Res. *665*, 20–28.

Munro, S., Oppermann, U., and La Thangue, N.B. (2014). Pleiotropic effect of somatic mutations in the E2F subunit DP-1 gene in human cancer. Oncogene *33*, 3594–3603.

Muotri, A.R., Marchetto, M.C., Coufal, N.G., Oefner, R., Yeo, G., Nakashima, K., and Gage, F.H. (2010). L1 retrotransposition in neurons is modulated by MeCP2. Nature *468*, 443–446.

Peters, A.H., Kubicek, S., Mechtler, K., O'Sullivan, R.J., Derijck, A.A., Perez-Burgos, L., Kohlmaier, A., Opravil, S., Tachibana, M., Shinkai, Y., et al. (2003). Partitioning and plasticity of repressive histone methylation states in mammalian chromatin. Mol. Cell *12*, 1577–1589.

Roulois, D., Loo Yau, H., Singhania, R., Wang, Y., Danesh, A., Shen, S.Y., Han, H., Liang, G., Jones, P.A., Pugh, T.J., et al. (2015). DNA-demethylating agents target colorectal cancer cells by inducing viral mimicry by endogenous transcripts. Cell *162*, 961–973.

Schlesinger, S., and Goff, S.P. (2015). Retroviral transcriptional regulation and embryonic stem cells: war and peace. Mol. Cell. Biol. *35*, 770–777.

Slotkin, R.K., and Martienssen, R. (2007). Transposable elements and the epigenetic regulation of the genome. Nat. Rev. Genet. *8*, 272–285.

Vormer, T.L., Wojciechowicz, K., Dekker, M., de Vries, S., van der Wal, A., Delzenne-Goette, E., Naik, S.H., Song, J.Y., Dannenberg, J.H., Hansen, J.B., et al. (2014). RB family tumor suppressor activity may not relate to active silencing of E2F target genes. Cancer Res. *74*, 5266–5276.

Walter, M., Teissandier, A., Pérez-Palacios, R., and Bourc'his, D. (2016). An epigenetic switch ensures transposon repression upon dynamic loss of DNA methylation in embryonic stem cells. eLife *5*, e11418.

Wells, J., Yan, P.S., Cechvala, M., Huang, T., and Farnham, P.J. (2003). Identification of novel pRb binding sites using CpG microarrays suggests that E2F recruits pRb to specific genomic sites during S phase. Oncogene *22*, 1445–1460.

Wylie, A., Jones, A.E., D'Brot, A., Lu, W.J., Kurtz, P., Moran, J.V., Rakheja, D., Chen, K.S., Hammer, R.E., Comerford, S.A., et al. (2016). p53 genes function to restrain mobile elements. Genes Dev. *30*, 64–77.

Yamasaki, L., Jacks, T., Bronson, R., Goillot, E., Harlow, E., and Dyson, N.J. (1996). Tumor induction and tissue atrophy in mice lacking E2F-1. Cell *85*, 537–548.

Yu, P., Lübben, W., Slomka, H., Gebler, J., Konert, M., Cai, C., Neubrandt, L., Prazeres da Costa, O., Paul, S., Dehnert, S., et al. (2012). Nucleic acid-sensing Toll-like receptors are essential for the control of endogenous retrovirus viremia and ERV-induced tumors. Immunity *37*, 867–879.